Geological Survey of Canada
Open File 7896

OUTCROPPING AND REMOTELY PREDICTED LINEAMENTS, FAULTS, FRACTURES, AND DYKES IN THE KIGGAVIK URANIUM CAMP, NUNAVUT

A. Anand[1] and C.W. Jefferson[1]

ABSTRACT

Reactivated faults and their intersections are key exploration criteria for unconformity associated uranium (U) deposits. This poster shows how lineament data were generated and compiled over the Kiggavik uranium (U) camp, Nunavut, as part of a larger goal to understand fault reactivation in and around the northeastern Thelon Basin. The remote predictive maps presented here show lineaments at various scales, from regional scale through to camp scale to highly detailed. We show how the fractal range of lineament scales can be connected to and calibrated from detailed outcrop exposures. Lineaments were added to the compilation based on single prominent, or two or more moderate but coincident, straight features and/or offsets of other linear features, such as: broad to narrow demagnetized zones, stepped changes from higher to lower aeromagnetic intensity, linear magnetic highs associated with dykes filling these faults, straight sections of streams, lake-shores and swamps, linear steps in elevation, and geological contacts. The orientations of parallel swarms of lineaments are used to assign lineaments to classes of structures consistent with Riedel shear stress models. The lineaments are interpreted as faults, fractures and shear zones that resulted from a long, episodic Proterozoic deformation history, presented herein abbreviated form. The structural geological rationales for linking the stress models to successive tectonic events are developed with outcrop examples in the simultaneously released Open File 7895.

Note: References cited in poster are located in accompanying digital file.

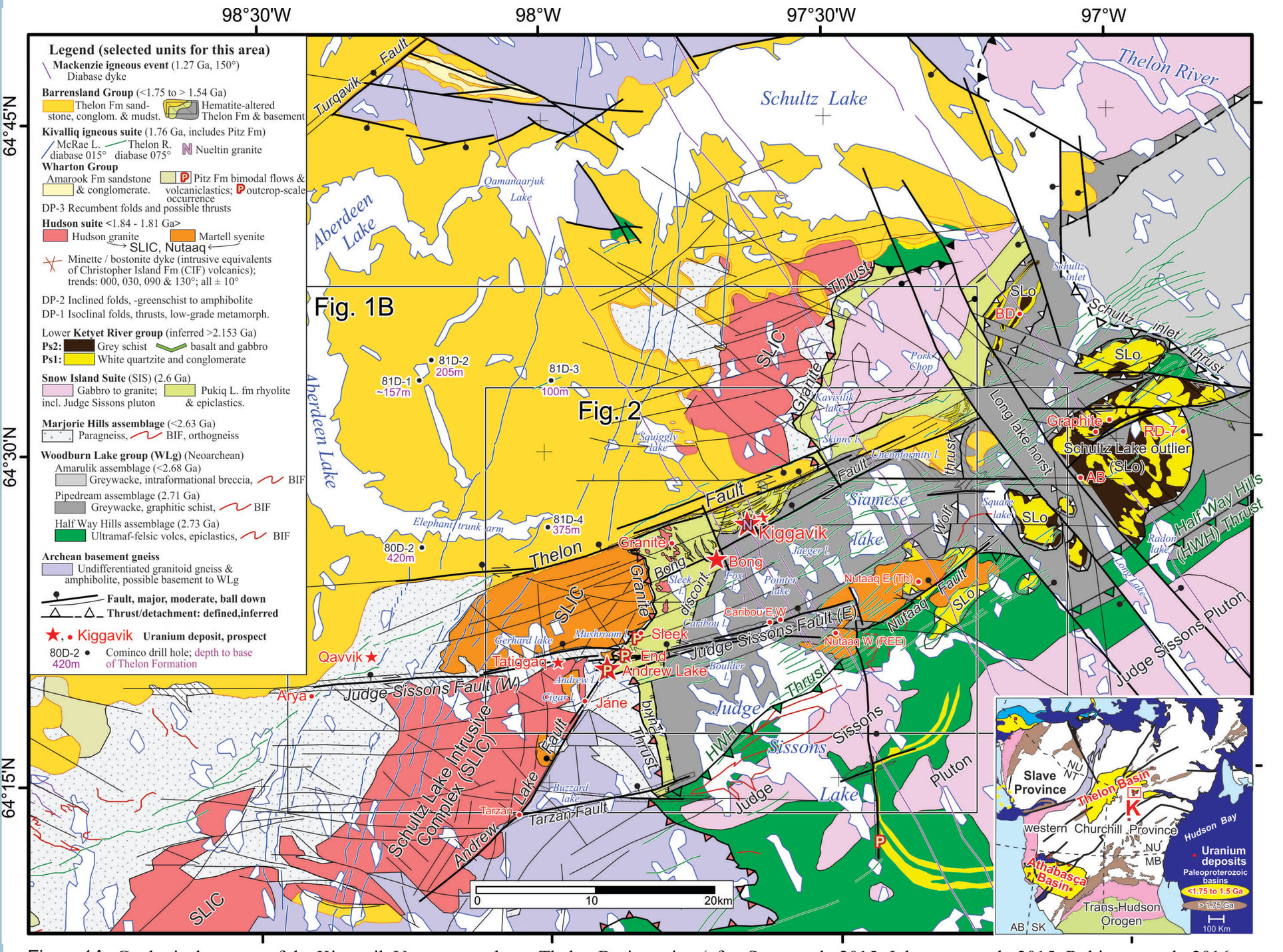

Figure1A. Geological context of the Kiggavik U camp, northeast Thelon Basin region (after Scott et al., 2015; Johnstone et al., 2015; Robinson et al., 2016; Jefferson et al., in prep. b). Box "K" in the inset map of the northwestern Canadian Shield shows the cratonic context. The Schultz Lake Intrusive Complex was petrologically defined by Miller and Peterson (2015) and restricted to west of Granite thrust by Tschirhart et al., (2013b). U occurrences are from Gandhi et al. (2015). Note: References cited in poster are located in accompanying digital file.

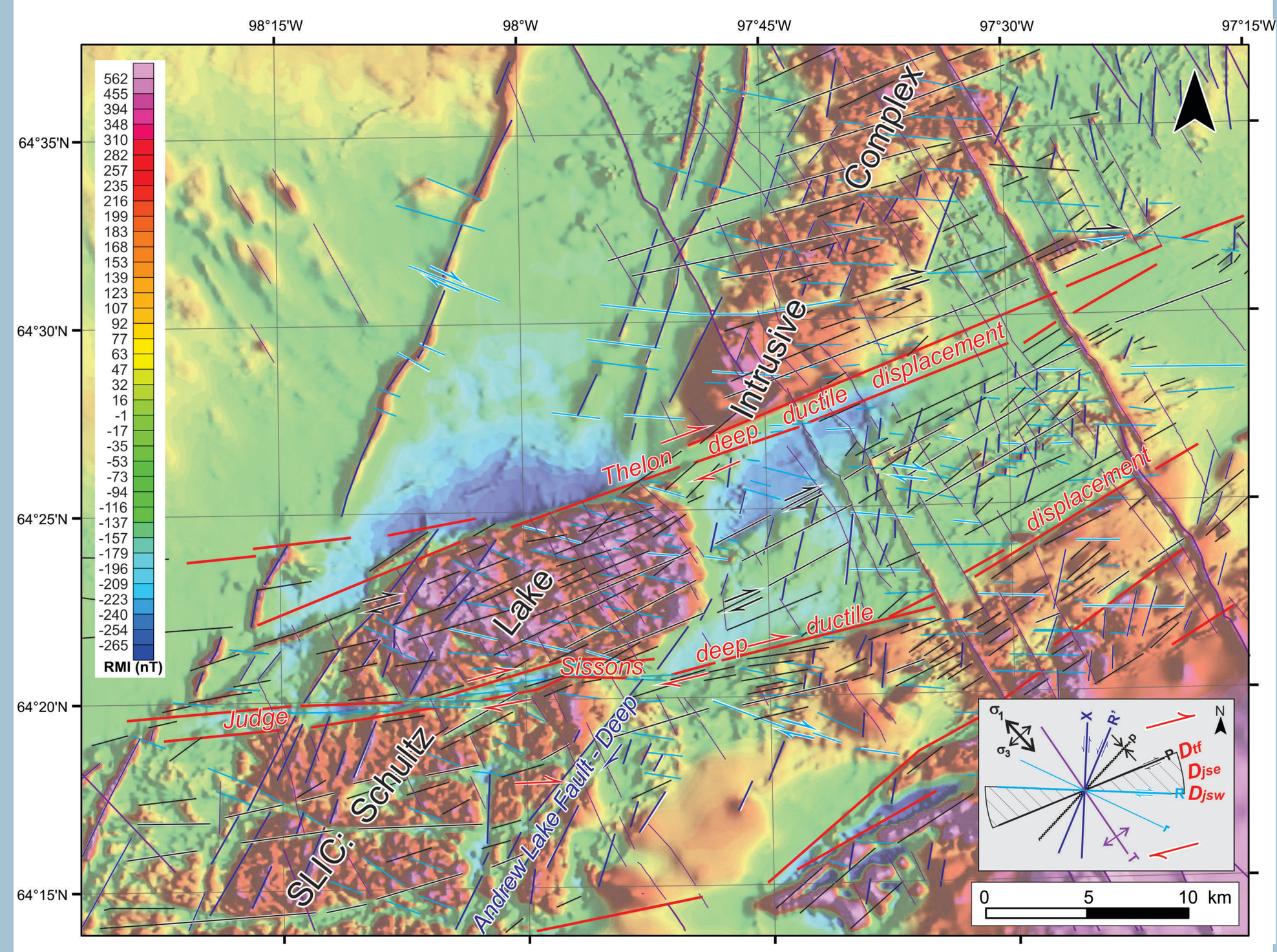

INTRODUCTION and ACKNOWLEDGMENTS

Reactivated faults, key for unconformity associated U deposits (Jefferson et al., 2007a, b, c), have long been recognized in this region (e.g. Fuchs et al., 1986; Fuchs and Hilger, 1989; Hunter et al., 2012; Jefferson et al., 2011b; Miller and LeCheminant, 1985; Miller and Peterson, 2015). Published maps and studies contain data, concepts and map pattens on which this project was built; e.g. the above and: Hadlari et al., (2004); LeCheminant and Roddick (1991); LeCheminant et al. (1983, 1984); Miller (1995); Patterson (1986); Pehrsson et al. (2004, 2013a); Peterson and LeCheminant, (1996); Peterson et al. (2002); Rainbird et al. (2003, 2006, 2010); Tella (1994); Tella and Heywood, (1978); Zaleski (2005); Zaleski and Pehrsson (2005). A new camp-scale structural analysis (Anand and Jefferson, 2017) considers <1% outcrop and drill data (the above; Johnstone et al., 2015; Jefferson et al., *in prep. b*), geophysical models (Tschirhart et al., 2011a, b; 2013a, b, c, d; 2014; 2016) and lineaments (herein). Detailed maps herein assign consistently oriented lineaments to classic strain elements based on a conceptual stress field model that evolved subtly through multiple events (Table 1).

Lineaments were mapped where very distinct and/or where two or more moderate lineaments coincide: broad to narrow demagnetized zones, stepped changes from higher to lower aeromagnetic intensity, linear magnetic highs associated with dykes (Figure 2A) filling these faults, straight sections of streams, lake shores and swamps, and linear steps in elevation. The lineaments were compiled on LANDSAT TM images, air photographs and total magnetic field images, and assigned to ideal strain element clusters (inset A of many figures). Assignments were based on orientation within about 15° of an ideal element direction. Local variations were considered, such as pre-existing anisotropies and relative positions of multiple arrays in a given locale. Strike-slip displacement directions were determined by offsets of other geological elements. Lineament names were derived from mainly informal topographic names. Thelon Fault Zone comprises a broad deep- seated demagnetized zone demarked by Felsenmeer lake and Ridge lake lineaments (brittle-ductile faults) on its NW and SE margins. Digital files included with this Open File, and incorporated in the figures shown here, were exported from an ArcGIS geodatabase.

High-resolution aeromagnetic, outcrop, and drill data were shared both digitally and through joint traverses and other personal collaborations under a consortium agreement among AREVA Resources Canada (P. Wollenberg, D. Quirt, D. Morrison, M. Blain,T. Riegler, and legacy Urangesellshaft data), Bayswater Uranium (G. Davidson and M. Muirhead), Cameco Corporation (G. Zaluski, R. Hunter, and G. Drever), Forum Uranium (K. Wheatley and A. Williamson), McMaster University (W.A. Morris and V. Tshirhart), GSC (listed in Jefferson et al., 2015), Mega Uranium (M. Downes and S. Kruse), NSERC, Nunavut Tunngavik Incorporated (C. Gilles, W. Johnson, and K. Morrison), Titan Uranium (R. Koch, P. Olson, P. Nicholls, M. McLaren, and B. Reilly), Uranium North (A. Armitage, M. Kolebaba, and R. Faasse), and Western Uranium (D. Bowden and P. Klessig). Industry sponsored theses, internal reports and publications provided key insights, including alteration histories such as early vs. late hydrothermal hematite and early silicification vs. late de-quartzification (Riegler, 2013; Riegler et al., 2014; Sharpe et al., 2015). Johnstone et al. (2015) greatly expanded knowledge and extent of Pukiq Lake formation epiclastic rocks. The following universities also contributed: Carleton (B. Cousens), Concordia (J. Patterson), Manitoba (M. Fayek), Nancy, France (M. Cuney), New Brunswick (A. LaRocque, B. Leblon, D. Lentz, and J.C. White), Queens (D. Layton-Matthews) and Regina (K. Bethune). Unpublished knowledge from A.R. Miller, S.J. Pehrsson, A.N. LeCheminant, P. Ramaekers, T. Skulski, and others guided the beginning of this project and is integral to these data. New geoscience from the NE Thelon GEM project included primary and derivative aeromagnetic images and other geophysical models (Thomas, 2012; Tschirhart et al., 2011a, b, 2013a, b, c, d, 2014, 2016); structural-metamorphic geology (Anand et al., 2012a, b; Calhoun et al., 2014; McEwan, 2012; Pehrsson et al., 2013a, b, 2014a, b); RADARSAT images and analyses (e.g. Shelat et al., 2011a, b; LaRocque et al., 2012); granite studies and adjacent geological maps (Miller and Peterson, 2015; Peterson et al. 2010, 2011, 2014, 2015a,b,c; Scott et al., 2015); drift prospecting (Robinson et al. (2014, 2016); and integrated mapping (Jefferson et al., 2011a, c, 2013, 2014, 2015, *in prep. a, b*). The Department of Indian and Northern Affairs Canada (K. Costello and B. MacIsaac), the Government of Nunavut (E. Prosh), the Canada Nunavut Geoscience Office (D. James and Dave Mate) and the Kivalliq Inuit Association (Veronica Tattuinee, P. Ag Luis Gerardo Manzo and staff) provided scientific and/or operational guidance and encouragement. GSC colleagues in Ottawa shared knowledge, discussed ideas and provided technical help: R. Buenviaje, L. Chorlton, W. Davis, A. Ford, S. Pehrsson, E. Potter, M. Sanborne-Barrie, and C. Stieber. Logistical support by Ookpik Aviation was contracted through Polar Continental Shelf Project, and Baker Lake Lodge (B. Kotelewetz) provided superior accommodation. Insightful critical reviews by Dr. K. Bethune with D. Johnstone (U of Regina) were most helpful, as were comprehensive scientific editing and input from D. Lemkow (GSC).

Table 1. Simplified structural evolution of the Kiggavik uranium camp.

Ga	Code	Event names	Kinematics and geological expression	References
?	DPh2	Post Ordovician extension	Multiple faults reactivated, Ordovician preserved in graben. Possible U remobilization	*Jefferson et al., (2015)*
0.447	DPh1	Ordovician marine transgression	Broad subsidence. Shallow marine platformal fossiliferous limestone	*Bolton and Nowlan (1979)*
1.04	DP12	Post-Grenville crustal relaxation	Mini-roll front U remobilization.	*Sharpe et al., (2015)*
~1.12	DP11	Grenville Orogeny	Thermal event. Partial re-setting of ages of U oxide minerals	*Sharpe et al., (2015)*
~1.27	DP10	Mackenzie dykes	Reactivated Bathurst faults from DP4 were common preferred zones of weakness followed roughly by the Mackenie dykes that radiated from the Coppermine plume.	*LeCheminant and Heaman (1989)*
<1.54	DP9	Deposition of Lookout Point Formation	Regional cratonic subsidence, marine transgression.	*Gall et al., (1992); Bridge et al., (2013); Sharpe et al., (2015)*
1.54	DP8	North American far-field compression; fault reactivation and highly focused, low-volume ultrapotassic mafic magmatism	Craton-scale subsidence, deposition of carbonaceous mudstone then dolostone, focused eruption of mafic ultrapotassic lavas (Kuungmi Formation) from intersecting reactivated DP4 faults: main Bathurst (T) and McDonald (P shears). Increased major horsts and grabens, silicification, calcification, U remobilization.	*Ramaekers pers. comm. 2007; Pehrsson pers. comm. 2011; aeromagnetic data in Tschirhart et al., (2011a)*
1.63-1.54	DP7b	Multiple reactivations; primary U mineralization inferred. 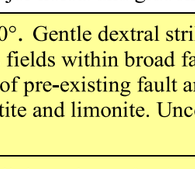	σ_1 ~120-140°. Gentle dextral strike slip and reactivated broad deep-seated fault zones; stress fields within broad faults are rotated ~10-20°; mostly extensional reactivation of pre-existing fault arrays. SiO_2 dissolution, bleaching, clay alterati on, earthy hematite and limonite. Unconformity U disseminated along DP1 & DP2 foliations.	*Fuchs & Hilger (1989); R. Hunter, oral presentation, Nunavut Mining Symposium, 5 April, 2011; Riegler et al., (2014); Sharpe et al., (2015)*
<1.68 - 1.63	DP7a		Gentle overall dextral reactivation of the fault arrays that were established & reactivated during DP4 through DP7, gentle drag folds adjacent to Thelon & Bong faults. U-bearing fluorapatite locally cemented Thelon Fm 1.68-1.67 Ga	*Davis et al., (2011); this map*
1.73 to 1.63	DP6b	Deposition of Thelon Formation	Regional thermal subsidence & broad gentle dextral trans-extension formed marked to subtle extensional sub-basins during overall subsidence. All fault arrays from DP4 & DP5 were reactivated, forming intersecting horsts and grabens. Lower Thelon Fm silicified along fault zones.	*Hiatt et al.,(2003); Davis et al. (2011)*
~1.73	DP6a	Hiatus	Broad and local uplift, subaerial erosion, oxidative paleoweathering, peneplanation	*Gall (1992)*
1.77 to ~1.73	DP5c	Kivalliq igneous suite	Dextral trans-extensional and normal reactivated surface faults follow DP2 and DP4 weaknesses. Regional counter-clockwise rotation of sequential dykes suggests clockwise craton rotation under dextral strain. Kivalliq Igneous Suite: bimodal intrusions and volcanics. Multiple hot to warm silicification, specular hematite, Ag-Au at Mallery Lake.	*Kivalliq Igneous Suite: Peterson et al. (2015a); Dp5c = late DP5 of Pehrsson et al., (2013a)*
1.785-1.77	DP5b	Wharton Group deposited	Overall thermal subsidence + dextral trans-extension reactivated most DP4 structures as dip-slip & extensional faults, forming sedimentary basins. Fluvial (coarse to fine) and aeolian siliciclastic rocks.	*DP5b =early DP5 of Pehrsson et al. (2013a)*
1.785-1.77	DP5a	Hiatus	Broad uplift, subaerial erosion & oxidative paleoweathering.	*Gall (1994); Rainbird et al., (2006)*
1.81 to 1.785	DP4b; over-lap DP3	Deposition of upper Baker Lake Group; major dextral fault systems, late Hudson suite granitoid magmatism.	Late Hudsonian reactivation of deep seated strike-slip systems: dextral-compressional with oblique reverse components. Deep-seated faults include: Amer Mylonite Zone, Amer Belt Medial Zone, Thelon Fault, Judge Sissons Fault & Nutaaq Fault. Hudson granitoid plugs at fault bends (Amer Plutonic Complex, Granite Grid, Lone Gull, Paliak Islands). Contact metamorphism with late Hudson granite in Kinngaaquk Core Complex. Calcite travertine @ 1785 +/-3 Ma pins upper Kunwak deposition	*=DP4 of Pehrsson et al., (2013a); Amer Plutonic Complex: Tella (1994); Jefferson et al., (2015); and Scott et al., (2015). Paliak granite (1.811 Ga) documented by LeCheminant et al., (1987). Travertine age from Rainbird et al., (2006).*
1.80 to 1.78	DP4a	Major thrust and/or regional structural discontinuity	East-directed Granite Thrust (or major north or west-verging regional detachment) juxtaposed exotic Marjorie Hills assemblage on 2.6 Ga Pukiq Lake fm.	*Tschirhart et al. (2013a, b); Jefferson et al. (2015; in prep. b)*
~1.82-1.78	DP3; over-lap DP4	Deposition of middle Baker Lake Group, main uplifts and exposure of Hudson suite granitoid exposures beside basins.	Early-Mid-Hudsonian SE-NW extension & unroofing caused subhorizontal chevron fold trains. Pressure drop & partial melting created mid-crustal granite sills filling dilation fractures possibly localized along earlier thrust or detachment planes. Main Hudson suite developed: granite + Martell syenite sheets to laccoliths partly inherit S2, filled weaknesses along translational structures. Calcite-chlorite-albite alteration associated with minette and bostonite dykes.	*Pehrsson et al., (2013a). Peterson et al., (2010), Rainbird et al. (2006), Scott (2012), Scott et al., (2015); van Breemen et al., (2005)*
~1.84-1.81	DP2b; over-laps DP3 & DP4	Main Hudsonian Orogeny: trans-extensional component; deposition of lower Baker Lake Group, main Hudson granitoid magmatism	Pull-apart basins along major dextral shear zones accommodated siliciclastic sedimentation (Baker Lake Group) and ultra-K volcanism (Christopher Island Formation minette to bostonite flows). The ultra-K magmas formed dykes in Kiggavik camp. Uraninite at Lac Cinquante is associated with Riedel shears, the basal unconformity of the Baker Lake Group, and calcite-chlorite-albite alteration.	*Peterson et al., (2010); Rainbird et al., (2006); Scott (2012); Scott et al., (2015); van Breemen et al., (2005). U references: Kazan: Stanton (1979); Lac Cinquante: Bridge et al., (2013)*
~1.85-1.83	DP2a	Main Hudsonian Orogeny: compressional component.	Basement-involved thick-skinned folds, reverse faults & thrusts, and klippes; Incipient mid-crustal partial melting starts producing Hudson granite	*Hadlari et al., 2004; Pehrsson et al., (2013a)*
~1.91 to 1.85	DP2a	Snowbird Orogeny; deposition of Ps4	Ps4 deposited in foreland basins northwest of this accretionary early Hudsonian event that welded the Hearn craton to the Rae.	*Jefferson et al. (2015); Pehrsson et al., (2013a); Zaleski et al., (2001)*
1.92 - 1.91		Hiatus	Tectonic quiescence except for local to regional uplift, erosion and weathering. Basal unconformity beneath Itza Lake formation truncates DP1 folds.	*Jefferson et al., (2015)*
~1.95-1.92	DP1a, DP1b DP1c	Proterozoic deformation	NE-directed, basement-involved thin-skinned translation, isoclinal & sheath folding, thrusts & décollements. Imbrication of rhyolite/epiclastic/quartzite units at Kiggavik. D1a/b/c phases (Calhoun et al., 2014) not distinguished around Kiggavik. Displacement was partitioned into domains separated by pre-existing dextral faults.	*Pehrsson et al., (2013a) and McEwan (2012); Calhoun et al., (2014)*
2.45-1.95		Lower Amer and Ketyet River groups (Ps0, 1,2,3) deposited	Broad to local subsidence with local extension reactivating previous dextral faults. Initial fluvial input transitioned to epeiric seas covering much of the Rae Craton.	*Rainbird et al., (2010); Bethune et al., (2013)*
<2.628		Deposition of Marjorie Hills assemblage	Marjorie Hills assemblage: coarse epiclastic turbidites, allochthonous because the 1-2 detrital zircon populations differ from the many of the Woodburn Lake group.	*Jefferson et al. (2014); McNicoll (2013, unpublished detrital zircon data)*
2.63-2.58	DA2b	Snow Island Suite & Pukiq Lake formation	Bimodal plutonic and volcanic magmatism intruded and covered much of the Rae Craton. Origin enigmatic, hypotheses include convergent plate margin with subduction, or within-crust post-orogenic to anorogenic event.	*LeCheminant and Roddick (1991); Pehrsson et al., (2013a); Peterson et al., (2015)*
	DA2a	Collisional deformation, polarity unknown	Cryptic pre-DP1 structures are locally preserved but cannot be interpreted due to Proterozoic overprints, possibly including Arrowsmith.	*Janvier et al., (2015)*
~ 2.76 to 2.68	DA2	Woodburn Lake group	Disparate Neoarchean components were formed and amalgamated in an island arc setting. Sedimentary components were eroded from diverse terranes of a micro-continent. Deformation and primary gold mineralization focused along faults bounding different assemblages.	*Ashton (1988); Davis and Zaleski (1998); Janvier et al., (2015); Pehrsson et al., (2013a); Zaleski et al., (2001); McNicoll (op. cit.)*
> 2.74	DA1	Inferred early shortening & thickening	Sanning and Akutuak River foliated tonalite either predated or were subvolcanic intrusions to early Woodburn Lake group. Cryptic locally preserved deformation.	*Schau et al., (1982); Davis and Zaleski (1998); Pehrsson et al., (2013)*

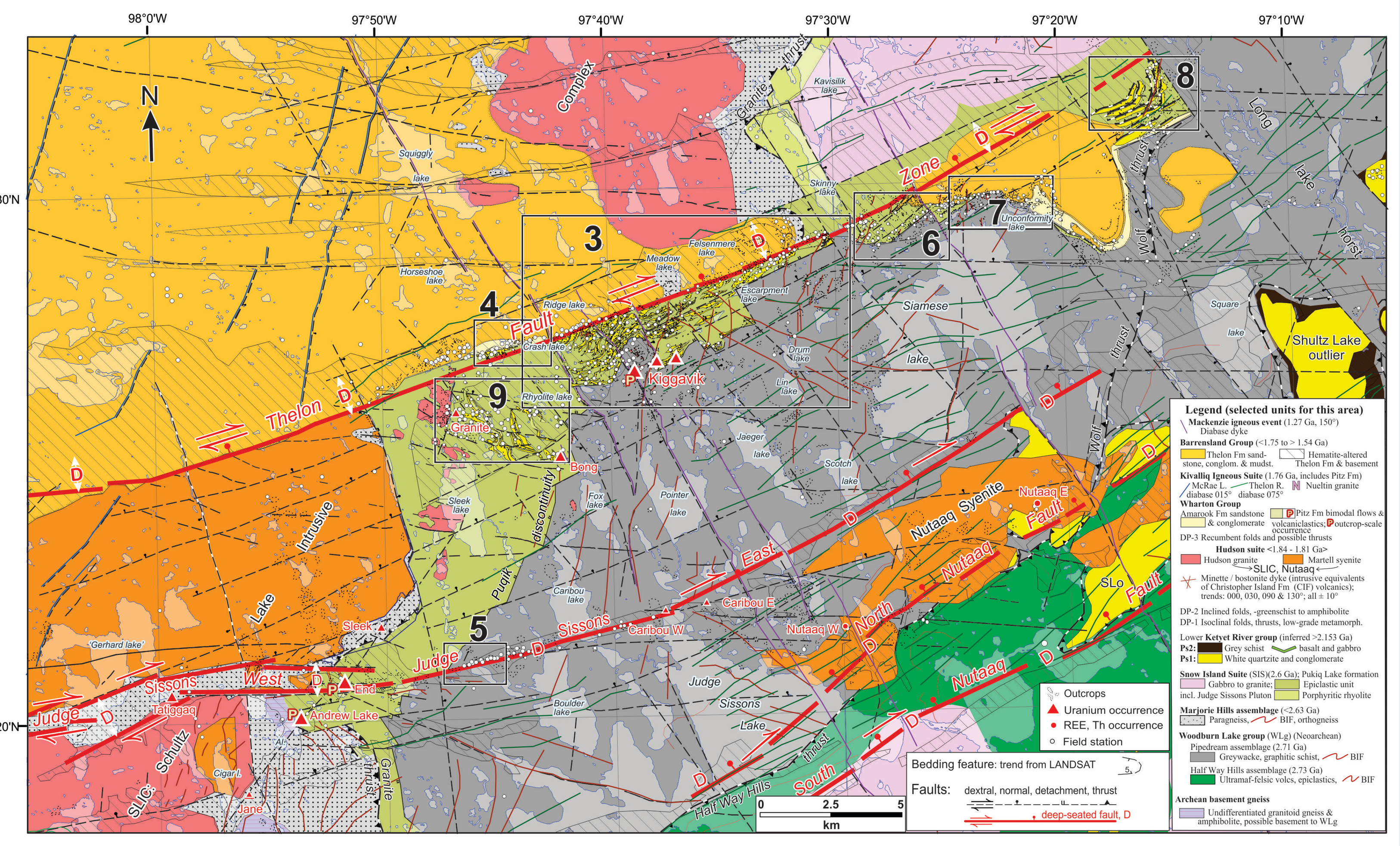

Figure 2A. Geological map of the Kiggavik uranium exploration area after Scott et al., (2015), Johnstone et al., (2015), Robinson et al., (2016) and Jefferson et al., (in prep. b). Locations of detailed lineament maps are shown by black boxes with numbers corresponding to figures in this poster. Dykes and major fault zones are the only linear features shown here; many of these are aligned with aeromagnetic lineaments shown below in Fig. 2B. Open circles are locations of outcrop data used in this study. Lake names are informal except for those with capitalized "Lake". Deep faults (D) are inferred from broad demagnetized zones and major steps in magnetic signature (Fig. 2B). Their surface expressions are discrete lineaments on one or both sides.

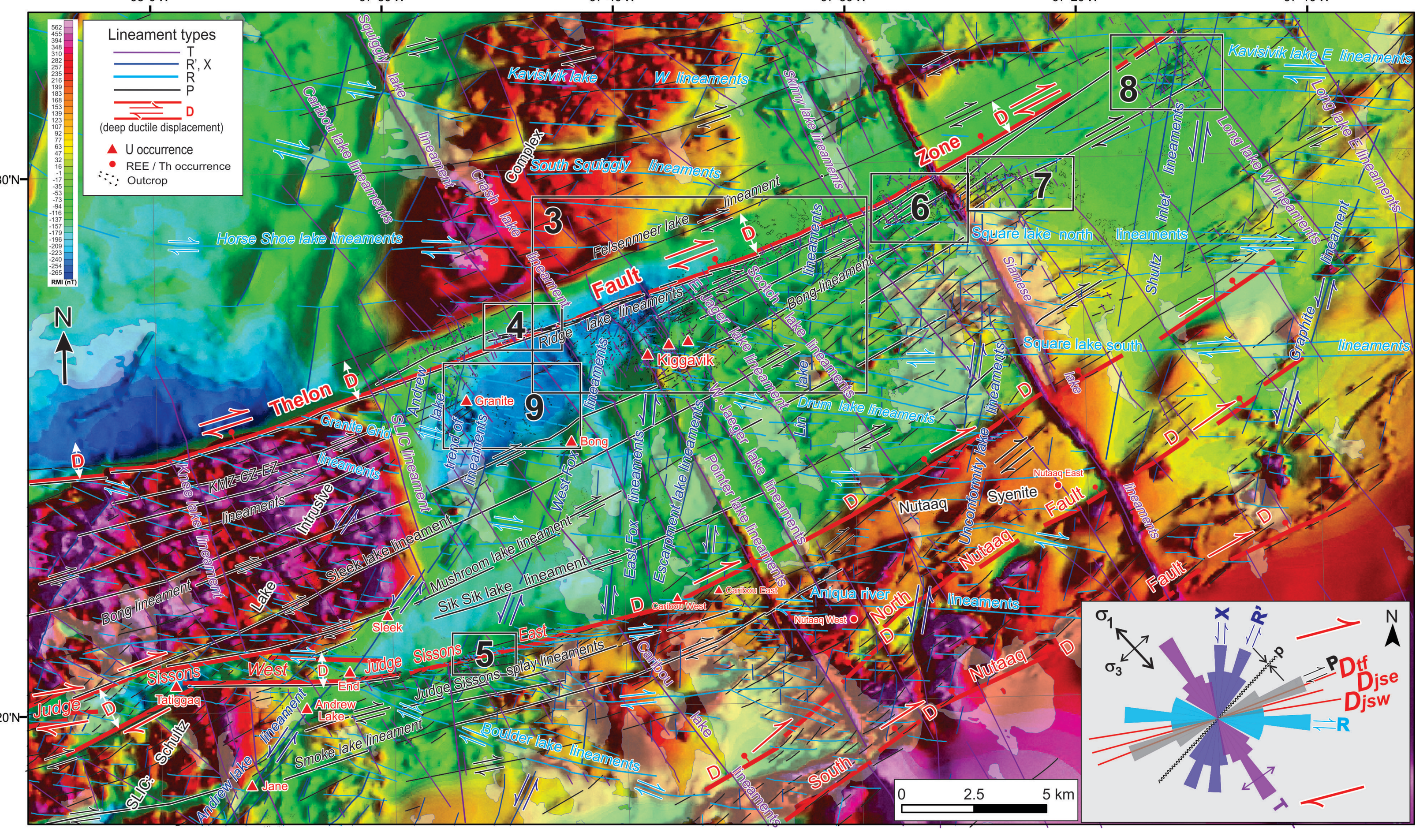

Figure 2B. Major lineaments in the context of regional airborne total magnetic field (image from Tschirhart et al., 2011a, b) in the same area as Figure 2A. The deep-seated ductile Thelon and Judge Sissons parent fault zones (D) are broad, deep demagnetized zones up to 1.5 km across (opposing white arrows) that are mostly covered by Thelon Formation and/or till respectively. Their southern and northern magnetic boundaries are shown by thick red lines here and in Figure 2A. Narrower lines coloured according to their orientations (key lower right inset) represent near-surface to surface lineaments derived from aeromagnetic, LANDSAT and other imagery. These lineament arrays represent secondary but still major brittle surface faults that fit into the Riedel shear model (inset, lower right). The observation that one or more lineaments of each array offset one to many lineaments of the other arrays supports the concept that these lineaments all developed or or were reactivated during roughly the same DP4 time period. Lakes (transparent) are labelled in Figure 2A.

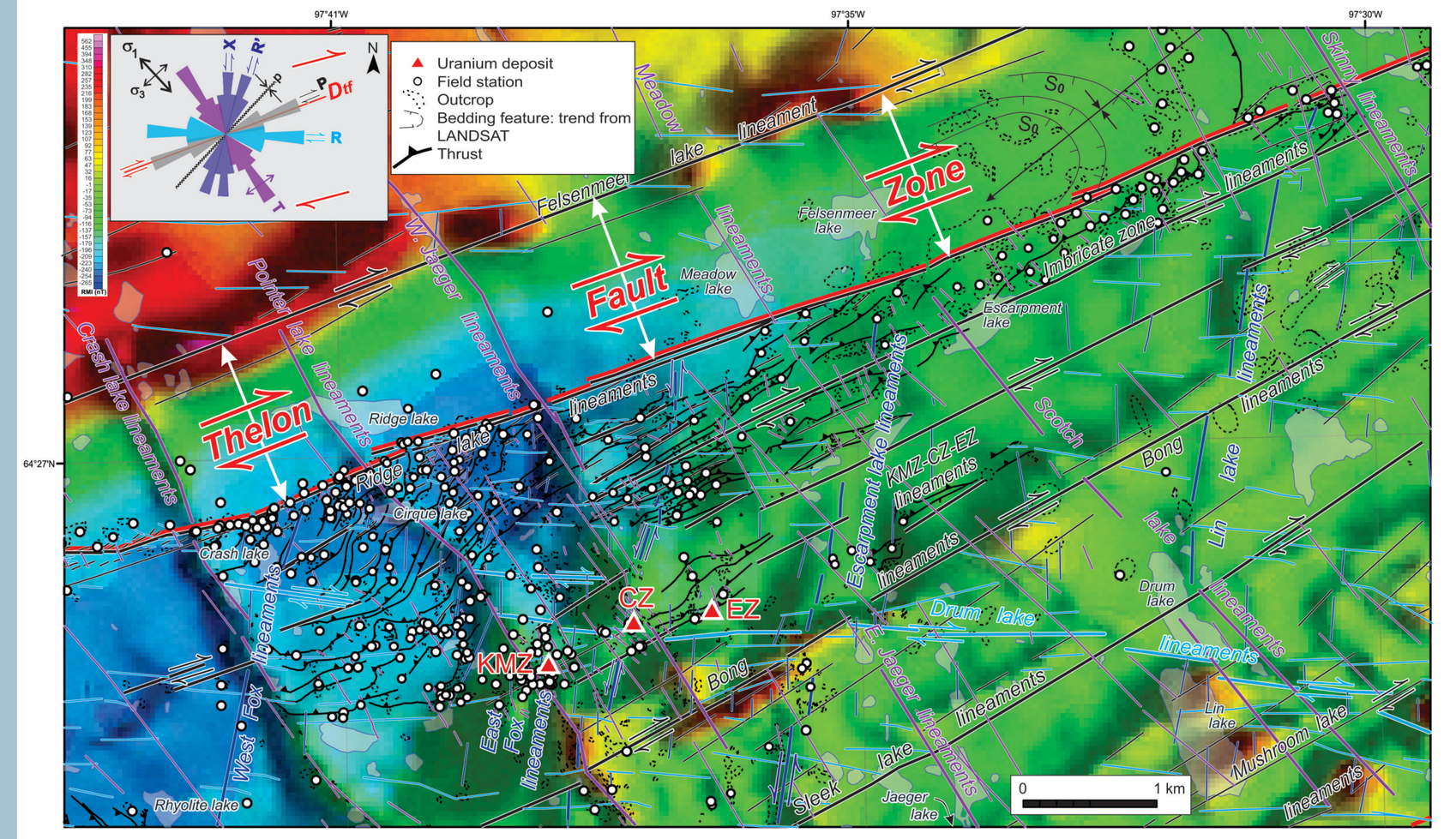

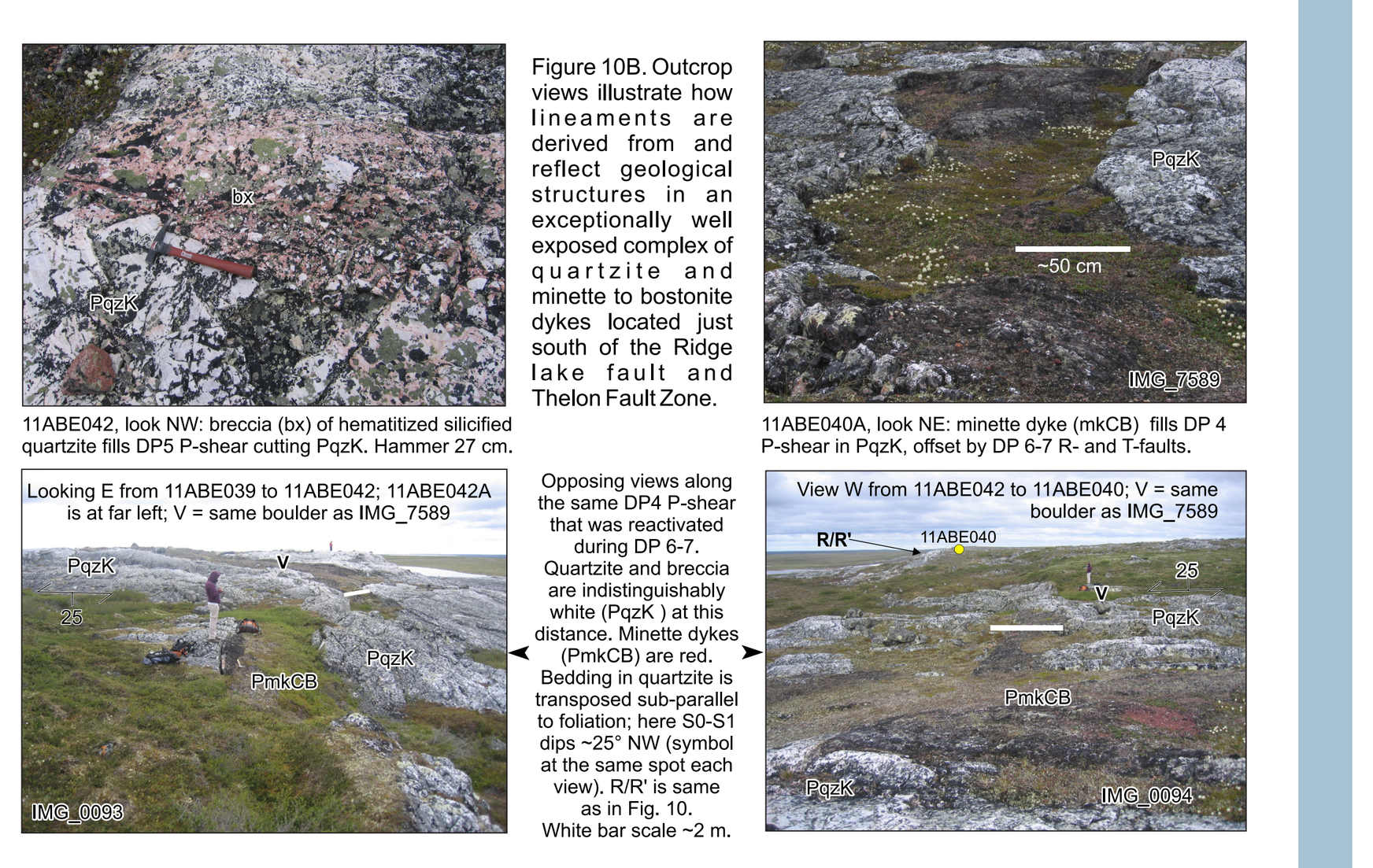

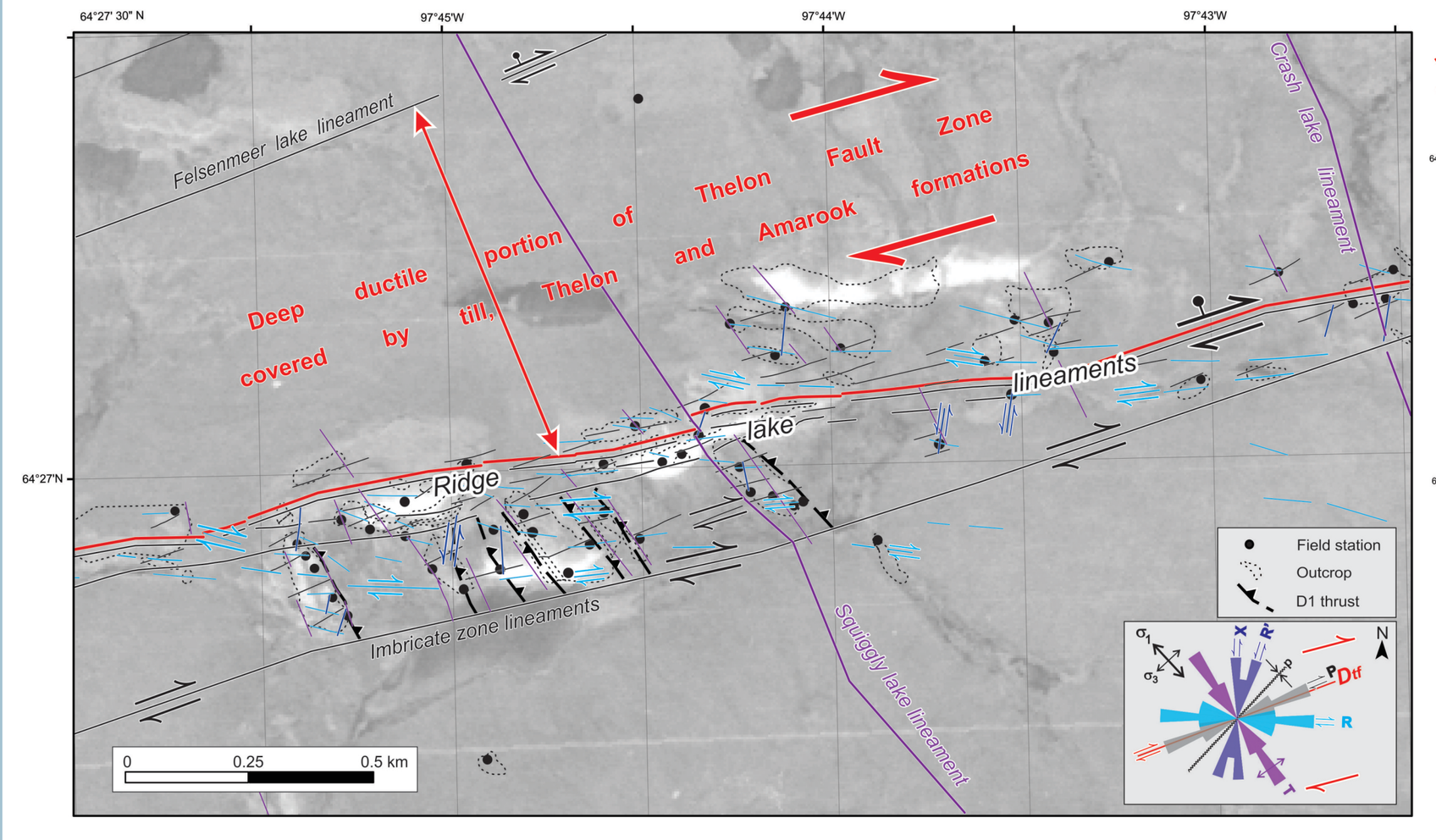

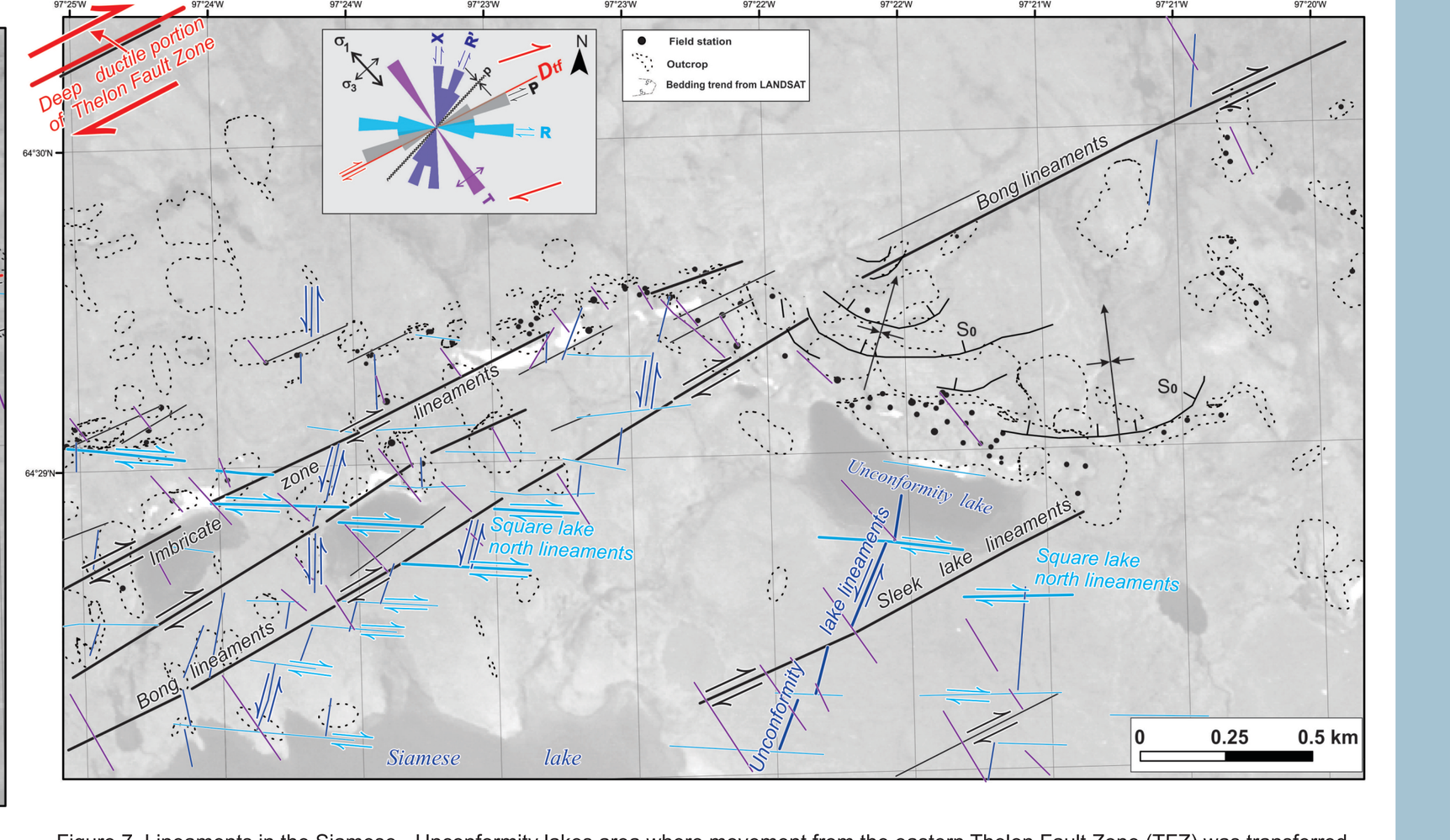

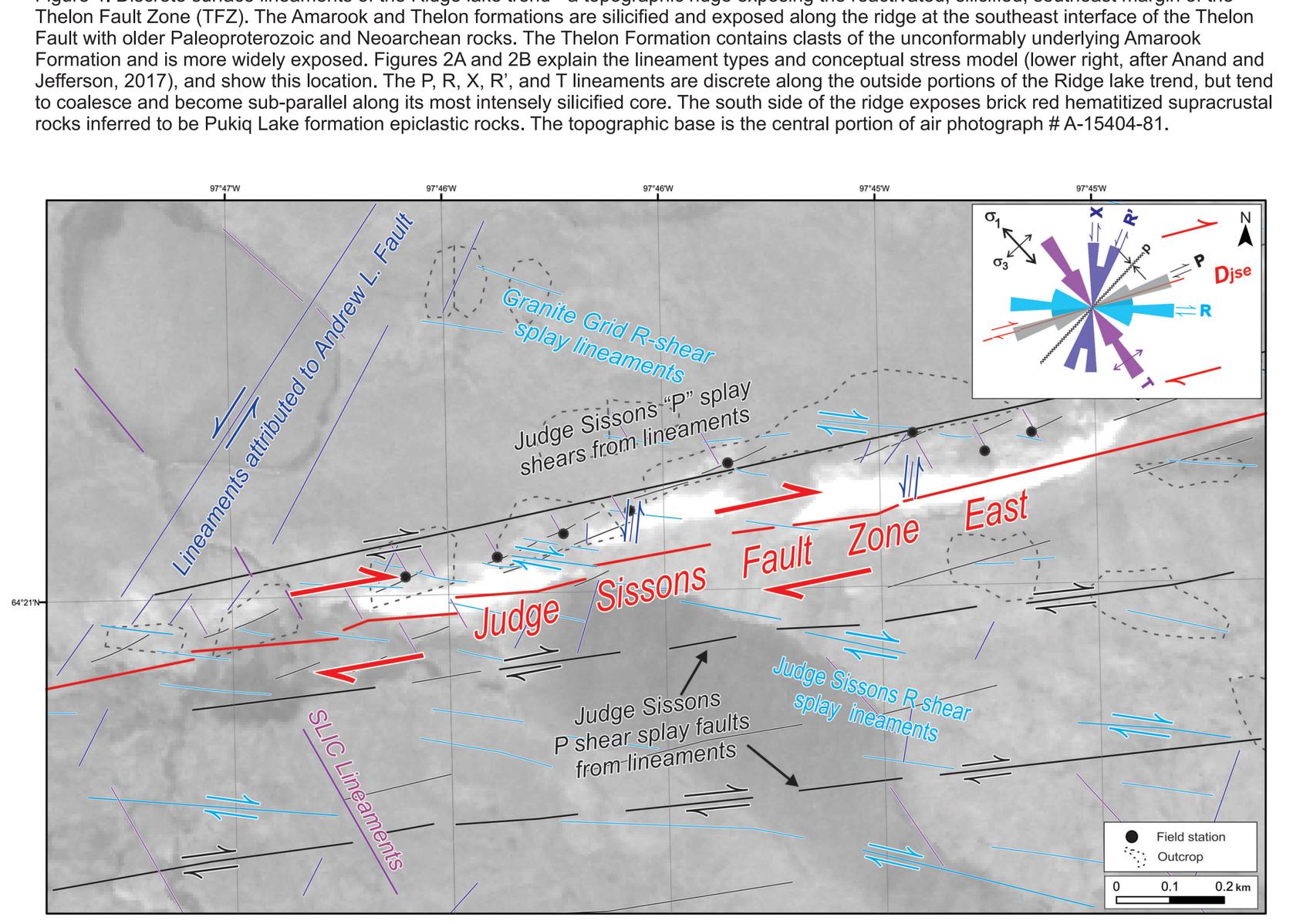

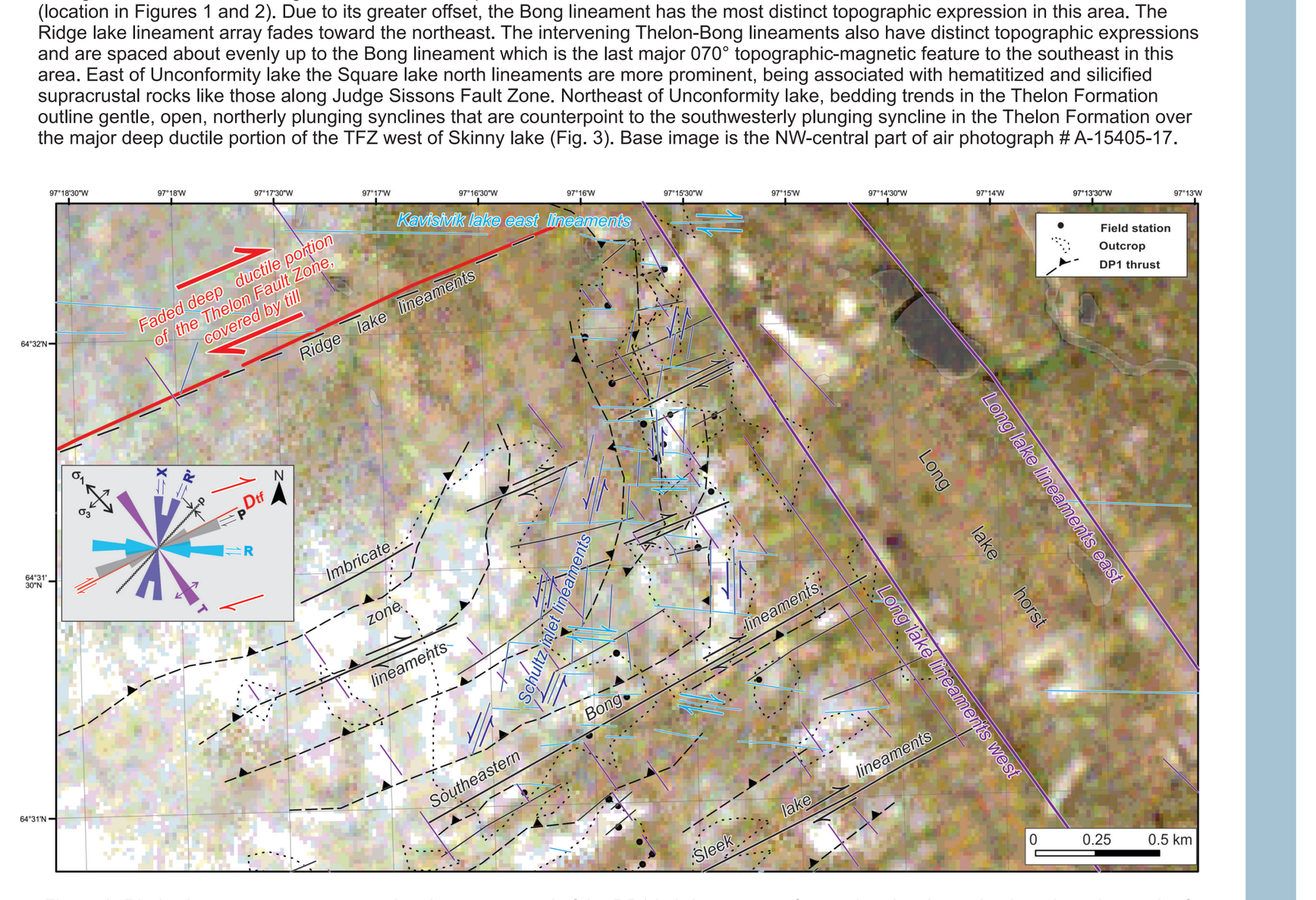

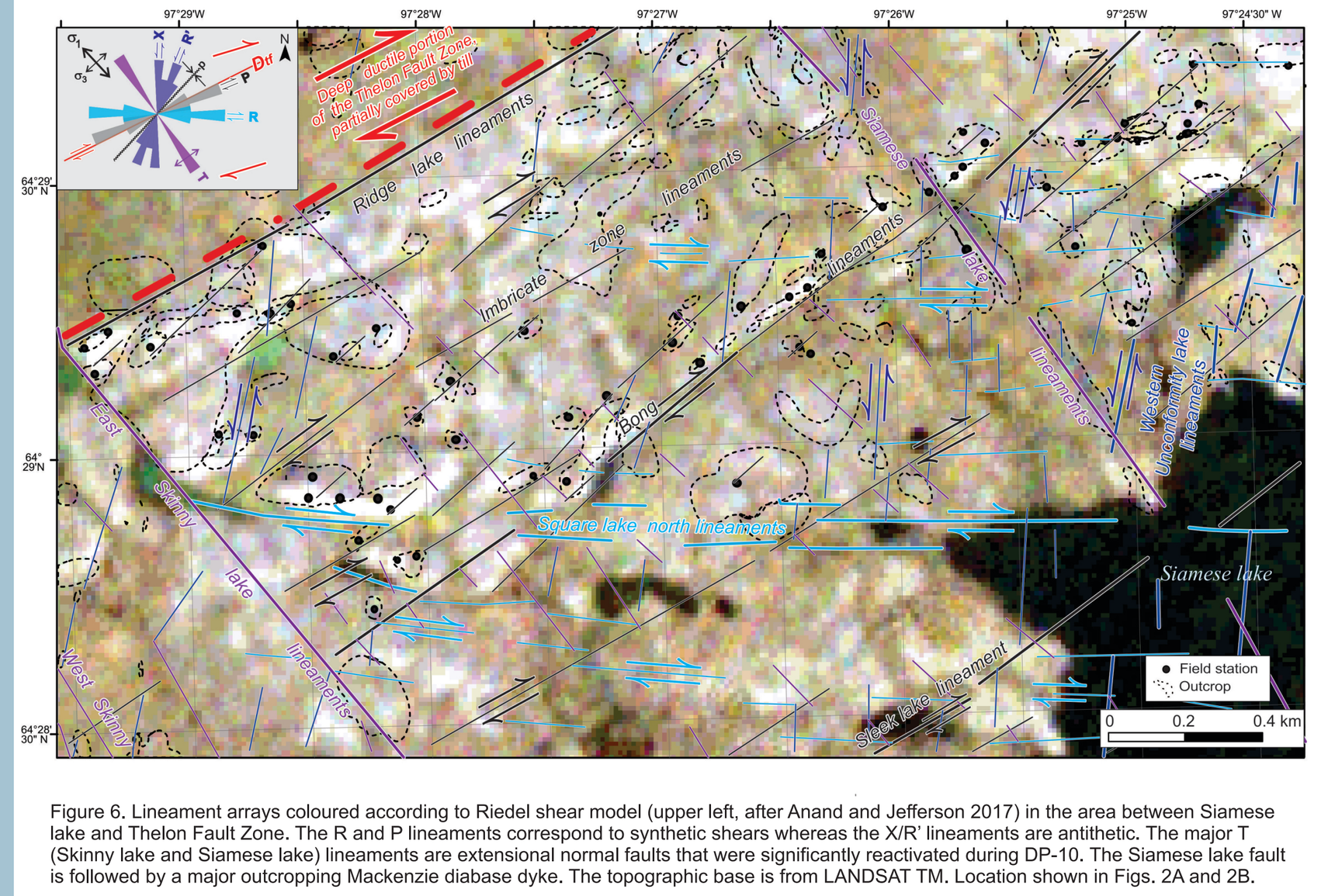

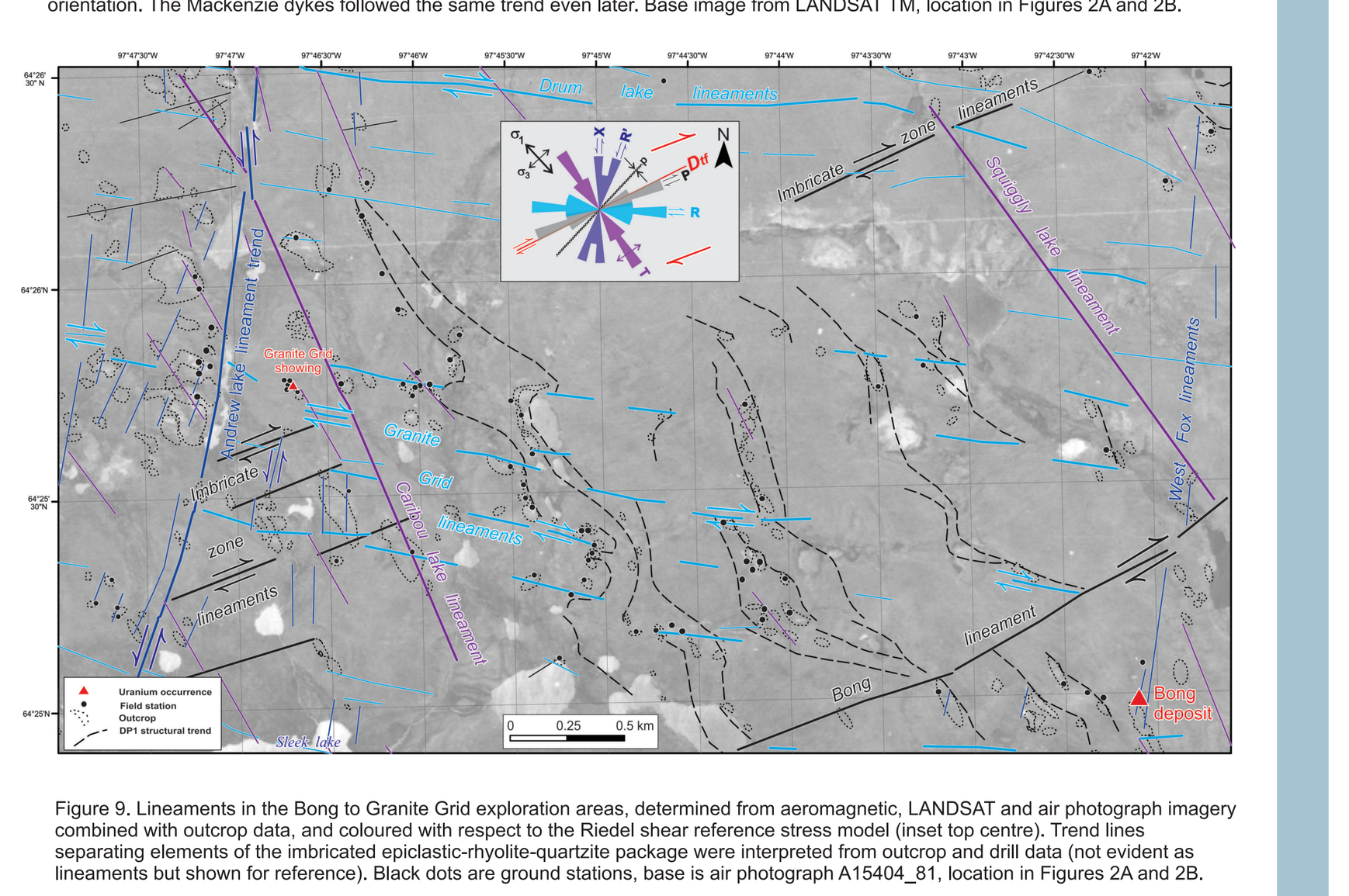

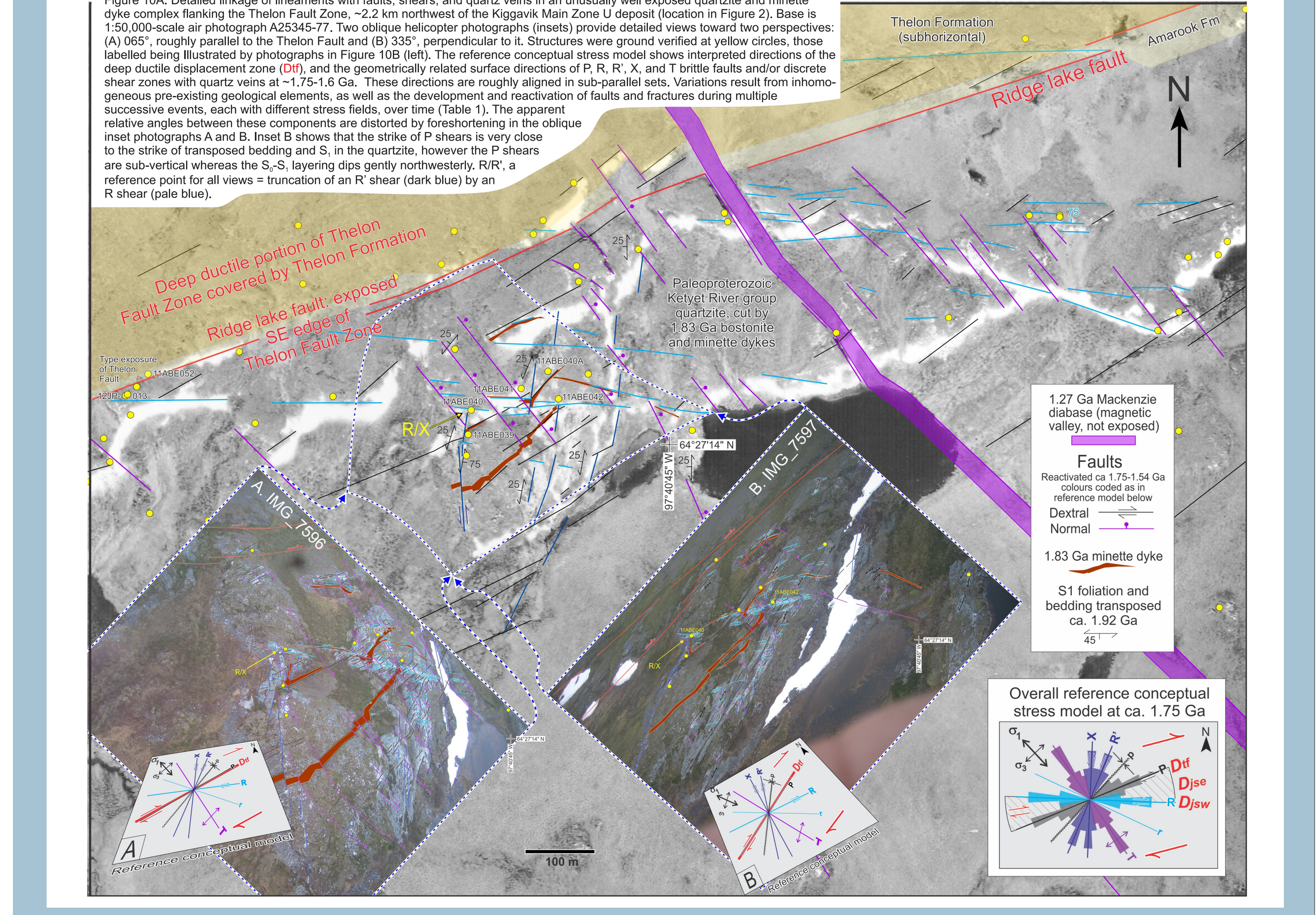

DISCUSSION AND CONCLUSIONS

Lineaments have been compiled and interpreted as faults by many previous workers in this region (e.g. LeCheminant et al., 1983; Tella, 1994; Hadlari et al., 2004; Miller and Peterson, 2015; unpublished lineament maps shared by consortium partners). As part of the GEM Uranium Project, predominantly aeromagnetic lineaments have been calibrated with LANDSAT, drill core logging (e.g. Davis et al., 2011) and outcrop data on regional scales to help map major units and more precisely locate and characterize fault structures in the northeast Thelon Basin Region (Jefferson et al., 2011a, c, 2013, 2014, 2015, *in prep. a, b*; Tschirhart et al., 2011a,b; 2013a,b,c,d; 2014; 2016).

This Open File presents the first part of a structural study under the GEM Uranium Project. This structural study organizes lineaments into preferred orientation sets and interprets them as faults and shear zones arranged according to the classic Riedel (1929) shear model as updated by Tchalenko (1970). We objectively mapped the lineaments using consistent criteria explained in the Introduction. Many of the more prominent lineaments were already documented as individual bedrock faults by the above-listed authors, but had not been interpreted in terms of Riedel shear. For the second part of this study Anand and Jefferson (2017) structurally assess the fault sets in the modern bedrock geological context.

This poster summarizes the lineaments in Figures 1B and 2B and provides representative detailed maps of them in Figures 3 to 10 inclusive. The lineament arrays are assigned to P, R, R', X, and T directions of the Riedel shear model as adapted to this area by Anand and Jefferson (2017). As noted in the Introduction many of the lineaments have a magnetic expression: in some cases demagnetized (e.g. Tschirhart et al., 2013c); in others a linear high due to dykes occupying the faults, as discussed below. The major demagnetized zones are broad bands with internal magnetic variations that are only faintly discernable at the resolution of our data. Both broad and narrow linear demagnetized bands are intensively hematitized and silicified, dequartzified and pervasively altered to clays and chlorite by hydrothermal processes as documented in drill core (e.g. Riegler, 2013; Riegler et al., 2014; Sharpe et al., 2015) and sparse outcrops. The low-magnetic bands are interpreted as deep ductile parent faults (D) that underlie high-level brittle-ductile deformed rocks such as the Thelon, Judge Sissons, and Andrew Lake faults. There are few outcrops of the deformed rocks because they are so altered and recessive, and therefore covered by Amarook and Thelon formations, and/or unconsolidated material. Very detailed ground magnetic data interpreted in terms of Riedel shear by Hunter et al., (2012) show that the same array of minor structures has affected the broad demagnetized zone of the western Judge Sissons Fault.

The southeast edges of the broadly demagnetized Thelon and Judge Sissons faults are well exposed as silicified ridges (e.g. the Ridge lake fault), as are some narrow brittle structures along the P, R, and R' trends. Silicification took place mainly during magmatism of the 1.75 Ga Kivalliq Igneous Suite (Peterson et al., 2015a), but later silicification of the altered zones also affected basal units of the Thelon Formation (<1.75 Ga) and was followed by introduction of fluorapatite cement at ca. 1.67 Ga (Davis et al., 2011).

Ground observations (e.g. Figure 10) document the lineaments as brittle-ductile to brittle and extensional faults, filled in places by magnetic minette, bostonite, and diabase dykes. The minette and bostonite dykes are part of the 1.83 Ga Christopher Island Suite (Peterson and LeCheminant, 1996; Peterson et al., 2002; Scott et al., 2015) which occupy all of the P, R, R/X', and T orientations, showing that the main structural framework had been established and these originally compressive structures had been reactivated extensionally in order to accommodate the ultrapotassic dykes.

The earliest diabase dykes are part of the 1.75 Ga Kivalliq igneous suite and occupy only the P, R, and R' orientations. The McRae Lake dyke swarm is traced as several linear to en échelon dykes beneath the northeast Thelon Basin and ~500 km farther northeast, via distinct linear aeromagnetic highs that correspond to mapped outcrops (Buchan and Ernst, 2013; Peterson et al., 2015b; Jefferson, et al., 2012). The R'-oriented McRae Lake lineaments are offset by R-oriented lineaments of the geochemically similar Thelon River dykes, just as R shears transect R' shears in outcrop (Fig. 10). The 1.27 Ga Mackenzie dykes (LeCheminant and Heaman, 1989) generate stronger and similarly continuous magnetic lineaments that record reactivation of the T structures, as they range from occupying to obliquely crosscutting and parallelling the T faults, slightly straightened clockwise from their predicted continent-scale radial pattern. The larger T faults bound horsts and grabens with throws from tens to hundreds of metres.

Although overall continuous, each fault and dyke in a given trend is en échelon rather than continuous. In many places step-overs are located where they cross other lineaments, strengthening fault interpretations. Early structures and dykes are offset by later ones, contributing to chronologic knowledge of faults and their relationships to tectonics (Table 1). Anand and Jefferson (2017) use such knowledge to understand complex internal geometries and predict favourable trends for uranium mineralization.

Figure 10 and accompanying ground photographs illustrate an unusually well exposed fault locality northwest of the Kiggavik deposits, includes a segment of the silicified brittle ductile Ridge lake fault that demarks the southern margin of the Thelon Fault Zone. This provides definitive examples of remotely mapped lineaments being located along discrete, en échelon, high-angle faults, breccias and shear zones in the P, R, R'/X, and T orientations. The lineaments and corresponding faults are fractal, with exposures in this locality guiding interpretation of the entire Kiggavik uranium camp and beyond. Crosscutting relationships of these lineaments, like the ground-mapped faults (Anand and Jefferson, 2017) generally show that P/R' conjugate sets were early, followed by P shears (e.g. P/R' in Figure 10).

The positive and negative magnetic lineaments that met the criteria of this study did so in large part because they correspond nicely with geological structures that have obvious surface and subsurface expressions, and provide geologically reasonable mapping solutions where exposure is poor. For example the distinct Shultz Lake Intrusive Complex (SLIC) that flanks the Kiggavik camp on the west is expressed as a broad aeromagnetic high with relatively abrupt margins on the east and west but highly dissected by demagnetized linear zones (Tschirhart et al., 2013b) that were recognized since the 1980s as fault zones (e.g. Urangeselleschaft unpublished maps; Fuchs et al., 1986; Fuchs and Hilger, 1989; Miller and LeCheminant, 1985; Miller and Peterson, 2015). The 0.1 to 2 km-diameter amoeboid granite plugs east of the SLIC were included undivided with the SLIC by previous workers, but separated as higher level discrete bodies by Tschirhart et al. (2013b). This distinction is supported by lineament analysis (Figures 1B, 2B).

In conclusion, rigorous lineament analysis that uses multiple data sets and ground-truthing produced geometrically consistent arrays with a high degree of predictability. These in turn represent faults as products of classic Riedel shear during overall dextral transpressive deformation. The structural models derived from these faults (Anand and Jefferson 2017) explain changing stress fields through successive alternating transpressive deformation (four main Paleoproterozoic events) vs. sedimentation and igneous events associated with dextral trans-extension (Table 1). Structural interpretation of lineament patterns integrated with ground-truthing helps to understand reactivation of deep-seated dextral strike-slip fault systems within Neoarchean supracrustal rocks that host all known significant uranium prospects in the area. This analysis provides relative spatial suggestions that structures initiated during DP4 and were reactivated many times during subsequent tectonic events. Aeromagnetic and outcrop data characterizing these subsequent events are discussed by Anand and Jefferson (2017).

This Open File release is a product of Natural Resources Canada's Geo-mapping for Energy and Minerals (GEM) program.

[1] Geological Survey of Canada